Supporting Information

Barberon et al. 10.1073/pnas.1100659108

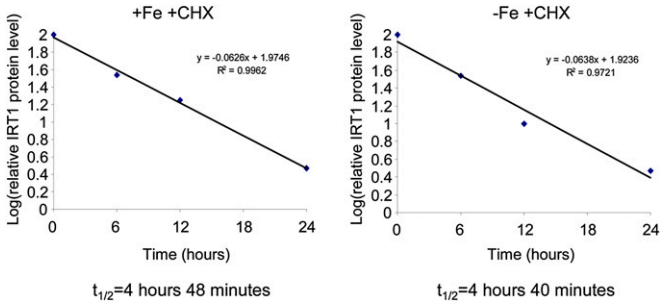

Fig. S1. Half-life of endogenous IRT1 protein. The data from Fig. 1*F* corresponding to the decay of IRT1 protein in the presence of CHX under the two iron regimes were log-transformed and fitted to a linear regression model.

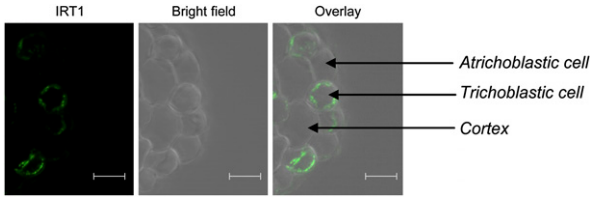

Fig. S2. IRT1 protein localizes to trichoblastic cells. Immunolocalization was performed using an anti-IRT1–specific antibody on root cross-sections from WT plants grown in iron-deficient conditions. The IRT1-specific signal and bright field are shown. The trichoblastic cell lineage lies over the cleft between two underlying cortical cells. (Scale bar = 10 μm.)

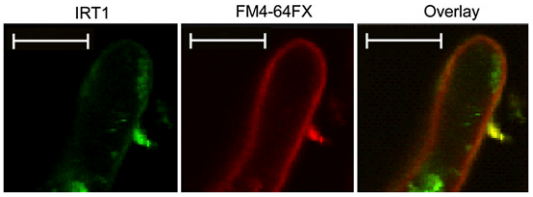

Fig. S3. IRT1-positive vesicles are distinct from the plasma membrane. Immunolocalization was performed using an anti-IRT1–specific antibody on roots from WT plants grown in iron-deficient conditions and subjected to staining with the fixable plasma membrane/endocytic tracer FM4-64FX. The whole-mount immunolocalization protocol has no effect on the plasma membrane structure. (Scale bar = 10 μm.)

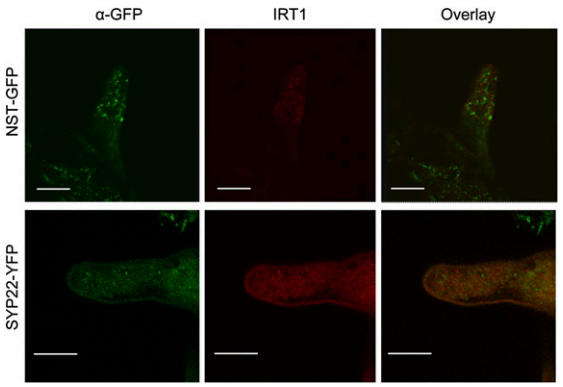

Fig. S4. IRT1 protein does not colocalize with Golgi and prevacuolar compartment markers. Whole-mount immunolocalization was performed on iron-deficient roots from NST-GFP and SYP22-YFP transgenic plants. Endogenous IRT1 does not colocalize with the Golgi-localized NST and the VAM3/SYP22 prevacuolar compartment/tonoplast-localized syntaxin protein. NST, nucleotide sugar transporter. (Scale bar = 10 μm.)

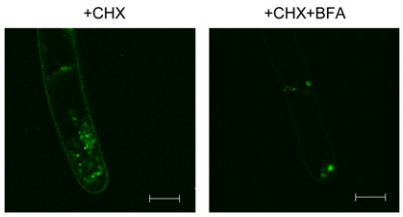

Fig. S5. IRT1 localizes to BFA compartments in the absence of de novo protein synthesis. Whole-mount immunolocalization was performed using the anti-IRT1 antibody on iron-deficient roots from WT plants treated for 30 min with CHX before BFA or mock treatment. Endogenous IRT1 protein localizes to BFA bodies in the absence of protein synthesis. (Scale bar = 10 μm.)

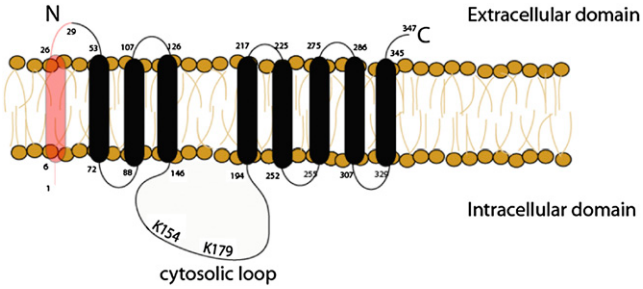

Fig. S6. Topology of IRT1 protein. IRT1 protein harbors a putative signal peptide (shown in red), followed by eight putative transmembrane domains. The positions of amino acids and the two lysine residues K154 and K179 are indicated.

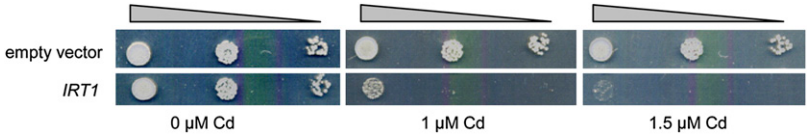

Fig. S7. Stable *IRT1* expression in yeast confers cadmium sensitivity. WT yeast expressing or not expressing IRT1 was grown in the presence of cadmium.

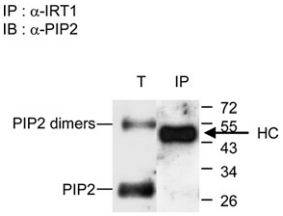

Fig. S8. IRT1 immunoprecipitates are specifically enriched in IRT1 protein. The abundant plasma membrane PIP2 aquaporin is not found in IRT1 immunoprecipitates. HC, heavy chain; IB, immunoblotting; IP, immunoprecipitation; T, solubilized root protein extracts.

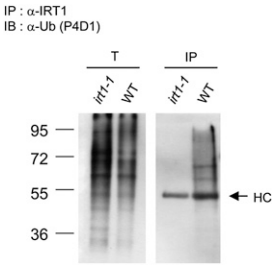

Fig. S9. IRT1 immunoprecipitates show ubiquitination signals using stringent solubilization conditions before IP. HC, heavy chain; IB, immunoblotting; IP, immunoprecipitation; T, solubilized root protein extracts.

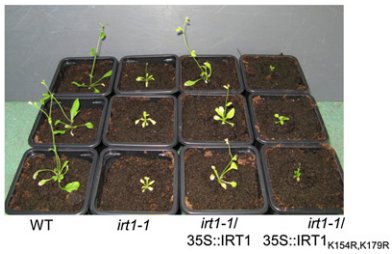

Fig. S10. Expression of IRT1K154R,K179R in *irt1-1* impairs plant growth, compared with plants expressing the WT form of IRT1, but still complements the chlorosis and the lethality of *irt1-1*. The *irt1-1*/35S::IRT1#9 and *irt1-1*/35S::IRT1K154R,K179R#1 lines are shown.

Table S1. List of primers used in this study

IRT1 FL F	AAGCTGCAGGAAAAAGCAGCAAAAGTTTTATTTA
IRT1 FL R	CGGGATCCACACAAACATTAAACAATCTAAAC
IRT1 K154R F	CTATACACCAGCAGGAACGCAGTTGGT
IRT1 K154R R	ACCAACTGCGTTCCTGCTGGTGTATAG
IRT1 K179R F	ACCTTACCAATAAGAGAAGATGATTCG
IRT1 K179R R	CGAATCATCTTCTCTTATTGGTAAGGT
IRT1 qPCR F	CGGTTGGACTTCTAAATGC
IRT1 qPCR R	CGATAATCGACATTCCACCG
APX1 qPCR F	TACGCTGCTGATGAAGATGC
APX1 qPCR R	GTTCAAATGCAATGCGACCC
EF1α qPCR F	GTCGATTCTGGAAAGTCGGACC
EF1α qPCR R	AATGTCAATGGTGATACCACGC

F, forward; qPCR, quantitative PCR; R, reverse.

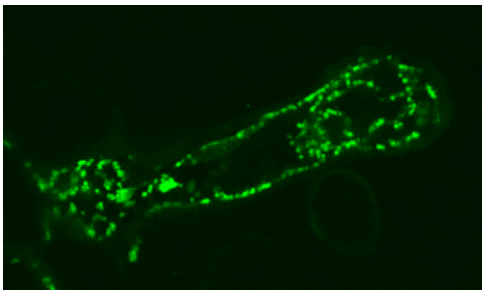

Movie S1. Z-stack analysis of an iron-deficient *Arabidopsis* root hair subjected to immunolocalization using an IRT1-specific antibody. Endogenous IRT1 localizes to intracellular vesicles in root hairs.

Movie S1